

# Investigations on the sine fitting algorithm in the Planck-Balance

*Shan Lin<sup>1</sup>, Christian Rothleitner<sup>1</sup>, Norbert Rogge<sup>2</sup>*

*<sup>1</sup>Physikalisch-Technische Bundesanstalt, Bundesallee 100, 38116 Braunschweig, Germany*

*<sup>2</sup>Institute of Process Measurement and Sensor Technology, Technische Universität Ilmenau, 98684 Ilmenau, Germany*

*shan.lin@ptb.de, christian.rothleitner@ptb.de, norbert.rogge@tu-ilmenau.de*

## Abstract

The Planck-Balance is a table-top version of a Kibble balance. In contrast to many other Kibble balances, the Planck-Balance generates an ac (sinusoidal) rather than a dc signal in the dynamic mode. A linear sine fitting algorithm is applied to estimate the amplitudes of the induced voltage and the coil motion, which determine the force factor  $Bl$  of the voice coil of the electromagnetic force compensated balance. Different sine fitting algorithms are compared in terms of harmonic distortion, additive Gaussian noise and non-coherent sampling. The biases and uncertainties associated with the estimated  $Bl$  are also compared by numerical simulations.

**Keywords:** Planck-Balance, three-parameter sine fit, multiharmonic sine fit, Monte Carlo simulation.

## Introduction

After the redefinition of the kilogram, the Kibble balance is one possible approach to calibrate mass standards in terms of a fixed value of the Planck constant [1]. The Kibble balance has two measuring modes: static mode and dynamic mode. In the static mode, the gravitational force on a mass  $m$  is balanced by an electromagnetic force that is generated by a voice coil, i.e.  $mg = BIl$ , where  $g$  is the local gravitational acceleration,  $I$  the electrical current,  $B$  the magnetic flux density and  $l$  the length of the coil-wire in the  $B$ -field. The product  $Bl$  is commonly called the force factor. In the dynamic mode,  $Bl$  is obtained by moving the coil with a velocity  $v$  through the magnetic field, while measuring the induced voltage  $u$  across the coil ends synchronously, i.e.,  $u = Blv$ . The  $Bl$  obtained in the dynamic mode is then used in the static mode to evaluate the mass  $m$  as a function of the coil current  $I$ .

The Planck-Balance (PB) is a table-top sized Kibble balance and is currently under development by the Physikalisch-Technische Bundesanstalt (PTB) and the Technische Universität Ilmenau (TUIL) [2]. In the dynamic mode of the PB, the coil is moved sinusoidally – in contrast to most other Kibble balance experiments, where the velocity is kept constant – through the  $B$ -field. If the coil motion is assumed to be perfectly sinusoidal, the velocity is simply the time derivative of the sinusoid. Therefore, the amplitude  $V$  of the velocity

becomes  $V = \omega S = 2\pi f_{\text{sig}} S$ , where  $S$  is the amplitude of the coil motion,  $\omega$  the angular frequency and  $f_{\text{sig}}$  the oscillation frequency. Then,  $Bl$  is calculated by dividing the amplitude of the induced voltage  $U$  by the amplitude of the velocity  $V$ , i.e.,  $Bl = U / (2\pi f_{\text{sig}} S)$ . However, this is strictly valid only if the coil motion and the induced voltage are perfectly sinusoidal. Therefore, the accuracy of  $Bl$  is influenced by the estimation of amplitudes, when perturbations, such as noise or distortions caused by non-linearities, are present in the signal.

In this paper, a linear sine fitting algorithm is applied with perturbations like, e.g., higher order harmonics, additive Gaussian white noise and non-coherent sampling. The resulting bias is investigated in numerical simulations. The standard uncertainty associated with the force factor  $Bl$  is evaluated by the GUM uncertainty framework and Monte Carlo simulation, respectively.

## Methodology

In dynamic mode of the PB, the coil sinusoidally oscillates through the  $B$ -field generated by the magnet system, and the coil position is measured by a laser interferometer. The movement of the coil induces an ac voltage across the coil ends, which is digitized by means of a multimeter. In the real measurement data of the induced voltage and the coil motion, higher order harmonics are present in the

signals after using Fourier analysis. Therefore, the signal of the induced voltage  $u(t)$  with time  $t$  can be described by using a single-component sine wave with amplitude  $U_1$  superimposed by higher order harmonics:

$$u(t) = U_0 + \sum_{n=1}^N U_n \sin(n\omega t + \varphi_{un}), \quad (1)$$

where  $U_n$  and  $\varphi_{un}$  are the amplitude and the initial phase of the  $n^{\text{th}}$ -order harmonic of the induce voltage, respectively.  $U_0$  denotes a dc offset, and  $N$  is the number of higher order harmonics, with  $N \in \mathbb{N}$ .

The coil motion  $s(t)$  can also be described by a sum of  $N$  harmonic terms:

$$s(t) = S_0 + \sum_{n=1}^N S_n \sin(n\omega t + \varphi_{sn}), \quad (2)$$

where  $S_0$  is a dc offset,  $S_n$  the amplitude of the  $n^{\text{th}}$ -order harmonic,  $\varphi_{sn}$  the phase of  $n^{\text{th}}$ -order harmonic.

The force factor  $Bl$  is calculated by using the signal frequency  $f_{\text{sig}}$  and the fundamental amplitudes of  $u(t)$  and  $s(t)$  as

$$Bl = \frac{U_1}{2\pi f_{\text{sig}} S_1}. \quad (3)$$

In the PB system, the signal frequency  $f_{\text{sig}}$  can be accurately achieved. Only the fundamental amplitudes  $U_1$  and  $S_1$  need to be estimated by the linear sine fitting algorithm. The following algorithms are applied to estimate the amplitudes:

- Three-parameter sine fit;
- Multiharmonic sine fit;
- Improved three-parameter sine fit.

Due to harmonic distortion in the measurement data, the accuracy of  $Bl$  is partly dependent on the fitting algorithm.

### Three-parameter sine fit

An ideal single-component sine wave can be described with an amplitude  $Y$  and an initial phase  $\varphi$  as:

$$y(t) = Y_0 + Y \sin(\omega t + \varphi) \quad (4)$$

where  $Y_0$  denotes a dc offset. Equivalently, the signal in Eq. (4) can be interpreted as a superposition of two shifted sine waves:

$$y(t) = Y_0 + A \sin(\omega t) + B \cos(\omega t) \quad (5)$$

where  $A$  and  $B$  are the amplitudes of in-phase and in-quadrature components, respectively. The signal frequency  $f_{\text{sig}}$  is assumed to be known in Eq. (5), and thus only three parameters  $Y_0$ ,  $A$  and  $B$  are required to be estimated. The estimated parameter vector  $\mathbf{p}$  can be represented as  $\mathbf{p} = [A, B, Y_0]^T$ .

When a set of  $M$  samples  $\{y_i\}_{i=1}^M$  from a sine wave is sampled at the time instants  $\{t_i\}_{i=1}^M$ , a linear least squares method can be used to

determine the parameter vector  $\mathbf{p}$  by minimizing the sum of the squares of the following errors:

$$\min_{A, B, Y_0} \sum_{i=1}^M (y_i - Y_0 - A \sin(\omega t_i) - B \cos(\omega t_i))^2. \quad (6)$$

The estimated parameters of the sine wave can be calculated in a matrix form:

$$\mathbf{p} = (\mathbf{D}^T \mathbf{D})^{-1} \mathbf{D}^T \mathbf{y} \quad (7)$$

with  $\mathbf{y} = [y_1 \ y_2 \ \dots \ y_M]^T$  and

$$\mathbf{D} = \begin{bmatrix} \sin(\omega t_1) & \cos(\omega t_1) & 1 \\ \sin(\omega t_2) & \cos(\omega t_2) & 1 \\ \vdots & \vdots & \vdots \\ \sin(\omega t_M) & \cos(\omega t_M) & 1 \end{bmatrix}. \quad (8)$$

The amplitude  $Y$  of  $y(t)$  can be calculated as:

$$Y = \sqrt{A^2 + B^2}. \quad (9)$$

### Multiharmonic sine fit

In the real measurement data of the induced voltage and the coil motion, higher order harmonics are present. These higher order harmonics may be caused, e.g., by the current source or the nonlinear  $B$ -field. However, the three-parameter sine fitting algorithm is not robust against the harmonic distortion with non-coherent sampling [3]. In order to improve the accuracy of the estimated amplitude, the multiharmonic sine fit has been proposed in [4]. The multiharmonic sine fit is the extension of the three- and four-parameter sine fit with the known and unknown signal frequency, respectively. In this paper, the linear optimization procedure based on the three-parameter sine fit is adopted.

When the signal contains higher order harmonic components, the signal is modeled by

$$y(t) = Y_0 + \sum_{n=1}^N Y_n \sin(n\omega t + \varphi_n), \quad (10)$$

where  $Y_n$  and  $\varphi_n$  are the amplitude and initial phase of the  $n^{\text{th}}$ -order harmonic, respectively. The fitting model for the linear least squares method can be written as follows:

$$y(t) = Y_0 + \sum_{n=1}^N [A_n \sin(n\omega t) + B_n \cos(n\omega t)], \quad (11)$$

where  $A_n$  and  $B_n$  are the  $n^{\text{th}}$ -order harmonic amplitudes of in-phase and in-quadrature components, respectively. By using the least squares method, the sum of the squares of the errors is minimized. The estimated parameters can be calculated to extend Eq. (7) as follows:

$$\mathbf{p}_m = (\mathbf{D}^T \mathbf{D})^{-1} \mathbf{D}^T \mathbf{y} \quad (12)$$

where  $\mathbf{p}_m$  is the parameter vector,  $\mathbf{p}_m = [A_1, B_1, \dots, A_N, B_N, Y_0]^T$ . Here,

$$\mathbf{D} = [\mathbf{S}_1 \ \mathbf{C}_1 \ \dots \ \mathbf{S}_N \ \mathbf{C}_N \ \mathbf{1}], \quad (13)$$

with

$$\mathbf{S}_n = [\sin(n\omega t_1) \quad \sin(n\omega t_2) \quad \cdots \quad \sin(n\omega t_M)]^T,$$

$$\mathbf{C}_n =$$

$$[\cos(n\omega t_1) \quad \cos(n\omega t_2) \quad \cdots \quad \cos(n\omega t_M)]^T,$$

$$n = 1, \dots, N.$$

The amplitude  $Y_n$  of the  $n^{\text{th}}$ -order harmonic of  $y(t)$  can be determined as:

$$Y_n = \sqrt{A_n^2 + B_n^2}. \quad (14)$$

### Improved three-parameter sine fit

Due to harmonic distortion, the conventional three-parameter sine fitting algorithm will provide a bias of the estimated amplitude for the non-coherent sampling. Multiharmonic sine fit is useful to estimate the amplitude of each order harmonic. The bias of amplitude is relatively low, when the number of higher order harmonics included in the fitting model approaches to that included in the measurement data. However, it is not easy to select the number for the fitting model.

An alternative method is to use a coherent sampling instead of the non-coherent sampling by removing some points at the beginning and/or at the end of the data, which makes the remaining points cover an integer number of periods of the sine wave.

Firstly, the first zero-crossing sampling point is detected, which satisfies the following equation:  $y(q_1 - 1) \cdot y(q_1) < 0$ . Here  $y(q_1) = y(t_{q_1})$  and  $q_1$  denotes the first index of the detected sample. The same routine is utilized to detect the other zero-crossing sampling points  $\{y(q_i)\}_{i=1}^{M_q}$ , where  $M_q$  is the total number of the detected samples. Then, some ending points are removed if they are not inside the following range:

$$y_i \notin \begin{cases} [y(q_1), y(q_{M_q} - 1)], & \text{if } M_q \text{ is odd} \\ [y(q_1), y(q_{M_q-1} - 1)], & \text{otherwise} \end{cases}. \quad (15)$$

Finally, the remaining points are extracted and used to estimate the amplitude by the three-parameter sine fit.

In practice, however, it is difficult to extract sampling points, which cover an exactly integer number of periods. Moreover, reduction of some samples can increase the bias and the standard deviation of the estimated amplitude [5]. If the number of samples is relatively large, the influence of reducing samples may be neglected in comparison to that due to harmonic distortion with non-coherent sampling. The simulation results will be shown in the following section.

### Uncertainty evaluation

All the sine fitting algorithms used in this paper are linear least squares models, and thus the standard deviations of the estimated parameters can be evaluated by using the covariance matrix  $\mathbf{V}$ . The expression is given in [6] as follows:

$$\mathbf{V} = \sigma_n^2 (\mathbf{D}^T \mathbf{D})^{-1}. \quad (16)$$

Here,  $\mathbf{D}$  is given by Eqs. (8) and (13) for the three-parameter sine fit and the multiharmonic sine fit, respectively.  $\sigma_n$  denotes the noise level of measurement. The result of  $\mathbf{V}$  can be presented in the following format:

$$\mathbf{V} = \begin{bmatrix} u(A_1, A_1) & u(A_1, B_1) & \cdots & u(A_1, Y_0) \\ u(A_1, B_1) & u(B_1, B_1) & \cdots & u(B_1, Y_0) \\ \vdots & \vdots & \ddots & \vdots \\ u(A_1, Y_0) & u(B_1, Y_0) & \cdots & u(Y_0, Y_0) \end{bmatrix}, \quad (17)$$

where  $u(p_i, p_j)$  is the covariance associated with estimates  $p_i$  and  $p_j$ .

The fundamental amplitude  $Y$  of the sine wave is calculated by using  $A_1$  and  $B_1$ , and thus only the covariances associated with  $A_1$  and  $B_1$  are used in the following steps. The submatrix  $\mathbf{V}_x$  extracted from the covariance matrix  $\mathbf{V}$  is

$$\mathbf{V}_x = \begin{bmatrix} u(A_1, A_1) & u(A_1, B_1) \\ u(A_1, B_1) & u(B_1, B_1) \end{bmatrix}. \quad (18)$$

According to the GUM uncertainty framework (GUF) [7], the standard uncertainty  $\sigma_y$  associated with the amplitude  $Y$  is given by:

$$\sigma_y^2 = \mathbf{C}_x \mathbf{V}_x \mathbf{C}_x^T, \quad (19)$$

where  $\mathbf{C}_x$  is the sensitivity matrix and evaluated as follows:

$$\mathbf{C}_x = \begin{bmatrix} \frac{\partial Y}{\partial A_1} & \frac{\partial Y}{\partial B_1} \end{bmatrix} = \begin{bmatrix} \frac{A_1}{\sqrt{A_1^2 + B_1^2}} & \frac{B_1}{\sqrt{A_1^2 + B_1^2}} \end{bmatrix}. \quad (20)$$

According to Eq. (19), the standard uncertainties  $\sigma_u$  and  $\sigma_s$  associated with the amplitudes  $U$  and  $S$  of the induced voltage and the coil motion can be deduced, respectively.

As mentioned before, the force factor  $Bl$  is calculated by using Eq. (3). The standard uncertainty  $\sigma_{Bl}$  associated with  $Bl$  is calculated by:

$$\sigma_{Bl}^2 = \mathbf{C}_{Bl} \mathbf{V}_{Bl} \mathbf{C}_{Bl}^T, \quad (21)$$

where  $\mathbf{C}_{Bl}$  and  $\mathbf{V}_{Bl}$  are the sensitivity matrix and covariance matrix for  $\sigma_{Bl}$  estimation, respectively. Here,

$$\mathbf{C}_{Bl} = \begin{bmatrix} \frac{\partial Bl}{\partial U_1} & \frac{\partial Bl}{\partial S_1} & \frac{\partial Bl}{\partial f_{sig}} \end{bmatrix},$$

$$\mathbf{V}_{Bl} = \begin{bmatrix} u(U_1, U_1) & u(U_1, S_1) & u(U_1, f_{sig}) \\ u(U_1, S_1) & u(S_1, S_1) & u(S_1, f_{sig}) \\ u(U_1, f_{sig}) & u(S_1, f_{sig}) & u(f_{sig}, f_{sig}) \end{bmatrix},$$

where  $u(U_1, U_1) = \sigma_u^2$  and  $u(S_1, S_1) = \sigma_s^2$ .

As the signal frequency can be accurately measured by a frequency counter ( $< 10^{-8}$ ), the term in Eq. (21) representing the signal frequency contribution to the uncertainty is neglected in this case. After a series of deduction, the relative standard deviation associated with  $Bl$  is:

$$\sigma_{Bl_{rel}} = \begin{cases} \sqrt{\frac{\sigma_u^2}{U_1^2} + \frac{\sigma_s^2}{S_1^2}}, & \text{if } u(U_1, S_1) = 0 \\ \sqrt{\frac{\sigma_u^2}{U_1^2} + \frac{\sigma_s^2}{S_1^2} - \frac{2u(U_1, S_1)}{U_1 S_1}}, & \text{otherwise} \end{cases} \quad (22)$$

### Numerical simulation of the relative bias of the amplitude

In order to investigate the influence of harmonic distortion on the  $Bl$  determination, the induced voltage and the coil motion are required to be simulated.

Firstly, the induced voltage is simulated by using a fundamental sine wave with the amplitude  $U_{ref} = 0.3051$  V and superimposed by higher order harmonics up to 5<sup>th</sup>-order. The amplitudes of 2<sup>nd</sup>-order up to 5<sup>th</sup>-order harmonic are 0.45 mV, 62.9  $\mu$ V, 2.40  $\mu$ V and 1.92  $\mu$ V, respectively. The total harmonic distortion is 0.15 %. These parameters are obtained according to real measurement data [8]. In order to simulate the non-coherent sampling, the signal frequency  $f_{sig}$  is changed from 3.82 Hz to 4.02 Hz with the same number of samples  $M = 10^4$ , i.e., the sampling frequency  $f_s = 1$  kHz and the sampling time  $T = 10$  s. For each  $f_{sig}$ , a data set of induced voltage  $\{u_i\}_{i=1}^{10^4}$  is generated and taken as the nominal points. Three algorithms are applied to estimate the fundamental amplitude  $\hat{U}_1$ . For the multiharmonic sine fit, 1<sup>st</sup>-order up to  $N^{\text{th}}$ -order harmonics ( $N = 1, 2, 3$  and 4) are included in the model, respectively. When only 1<sup>st</sup>-order harmonic is included in the multiharmonic sine fit (i.e.,  $N = 1$ ), the algorithm is the same as the three-parameter sine fit. For error comparison of amplitude, the value of  $U_{ref}$  is taken as the reference value. The relative bias of the amplitude  $\varepsilon_u$  is calculated, as  $\varepsilon_u = |\hat{U}_1 - U_{ref}|/U_{ref}$ . The results are shown in figure 1.

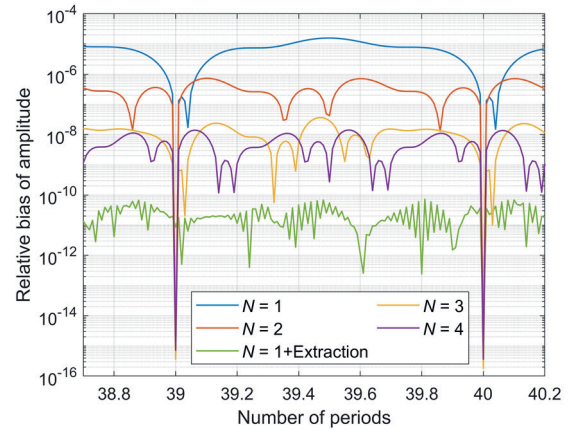


Figure 1: Relative bias of the amplitude as a function of the number of periods.

When the number of periods is an integer, i.e. coherent sampling, the amplitudes obtained from the three algorithms are comparable. Due to the numerical accuracy of the simulation data, the relative bias of the amplitude is in the order of  $10^{-15}$ . Therefore, the three algorithms are robust against harmonic distortion with coherent sampling. However, it can be seen that the relative bias of the amplitude provided by the three-parameter sine fit is in the order of  $10^{-6}$  with the non-coherent sampling. When the multiharmonic sine fit is applied, the higher the number of included harmonics is, the lower the bias of the estimated amplitude becomes. If higher order harmonics up to 5<sup>th</sup>-order ( $N = 5$ ) are included in the fitting model, there is no bias. The bias can greatly be reduced for the non-coherent sampling if the number of samples is reduced to obtain an integer number of periods (green line in figure 1).

Moreover, the coil motion is also simulated by using a fundamental sine wave with the amplitude  $S_{ref} = 39.92$   $\mu$ m and superimposed by higher order harmonics up to 5<sup>th</sup>-order. The amplitudes of 2<sup>nd</sup>-order up to 5<sup>th</sup>-order harmonic are 32.29 nm, 2.93 nm, 0.14 nm and 0.13 nm, respectively. The total harmonic distortion is 0.08 %. Similar to the induced voltage, the data set  $\{s_i\}_{i=1}^{10^4}$  of the coil motion is generated for each  $f_{sig}$ . Three algorithms are used to estimate the fundamental amplitude  $\hat{S}_1$  of the coil motion. Then,  $Bl$  is determined from the estimated amplitudes, i.e.,  $\hat{Bl} = \hat{U}_1 / (2\pi f_{sig} \hat{S}_1)$ . For error comparison, the fundamental amplitudes  $U_{ref}$  and  $S_{ref}$  in the simulated signals are used for the definition of the reference value of  $Bl$ , i.e.,  $Bl_{ref} = U_{ref} / (2\pi f_{sig} S_{ref})$ . Finally, the relative deviation of the calculated  $\hat{Bl}$  with respect to the reference  $Bl_{ref}$  is calculated, as  $\varepsilon_{Bl} = |\hat{Bl} - Bl_{ref}|/Bl_{ref}$ . The simulation results are presented in figure 2.

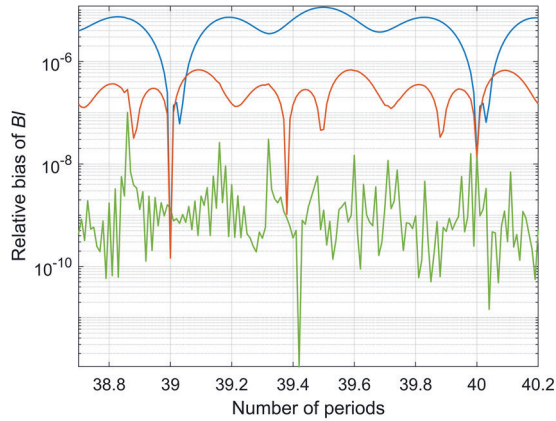


Figure 2: Relative bias of  $Bl$  as a function of the number of periods. The amplitudes are estimated by three-parameter sine fit (blue line), multiharmonic sine fit ( $N = 2$ , red line) and improved three-parameter sine fit (green line), respectively.

Similar results can be seen in figure 2: harmonic distortion with coherent sampling has almost no influence on  $Bl$  determination. However, when non-coherent sampling occurs, the three-parameter sine fit show the highest bias of  $Bl$ . Compared to the three-parameter sine fit, the multiharmonic sine fit ( $N = 2$ ) can reduce the bias of  $Bl$ . If an integer number of periods is extracted from the non-integer number of periods by deleting some ending points, the bias can be greatly reduced.

### Numerical simulation of standard deviation of amplitude

In this section, the GUM uncertainty framework (GUF) and the Monte Carlo method (MCM) are used to estimate the standard deviation of  $Bl$ . For the signal simulation, the nominal points  $\{u_i\}_{i=1}^{10^4}$  of the induced voltage and  $\{s_i\}_{i=1}^{10^4}$  of the coil motion are the same as those in the former section.

Firstly, the GUF is applied to estimate the relative standard deviation of  $Bl$  according to Eq. (22). According to one set of real measurement data, the standard deviations of noise are  $\sigma_{nu} = 0.1036$  mV for the induced voltage and  $\sigma_{ns} = 1.8768$  nm for the coil motion. The induced voltage and coil motion are measured by independent instruments, and here it is assumed that they are uncorrelated, i.e.  $u(U_1, S_1) = 0$ . The estimated relative standard deviation of  $Bl$  is shown in figure 3.

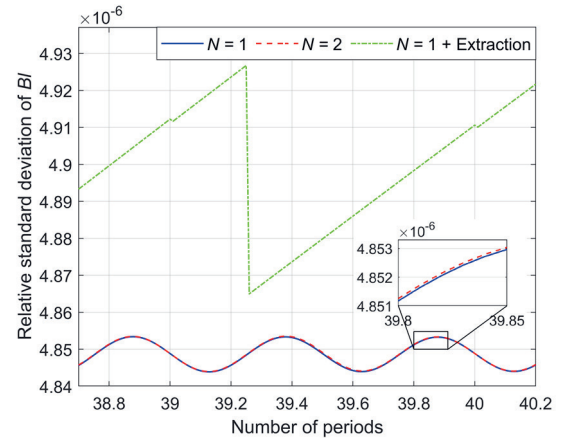


Figure 3: Relative standard deviation of  $Bl$  as a function of the number of periods. The amplitudes are estimated by three-parameter sine fit (blue line), multiharmonic sine fit ( $N = 2$ , red line) and improved three-parameter sine fit (green line), respectively.

In figure 3, all the relative standard deviations are in the same order of magnitude (i.e.,  $10^{-6}$ ). The improved three-parameter sine fit achieves the highest standard deviation. That is because the reduction of some samples increases the standard deviation of estimated amplitude. Therefore, the relative standard deviation of  $Bl$  is increased in the order of  $10^{-8}$ . If type A evaluation of standard uncertainty is applied, the relative uncertainty ( $k = 1$ ) is increased in the order of  $10^{-10}$ , which is much smaller than the accuracy aimed for the PB (about  $10^{-8}$ ). For the other two algorithms, the blue and red lines are almost indistinguishable, and the difference between them is in the order of  $10^{-10}$ . Moreover, when the non-coherent sampling occurs, the change of relative standard deviation is in the order of  $10^{-9}$ , which is also much smaller than the aimed accuracy of the PB. Therefore, the influence of non-coherent sampling on the standard deviation of  $Bl$  can be neglected. In practice, the amplitudes  $U_1$  and  $S_1$  are correlated according to the data analyzed in a real measurement, and the correlation coefficient is about -0.06. Compared to the uncorrelated amplitudes  $U_1$  and  $S_1$ , the acquired relative standard deviation is in the order of  $10^{-8}$  higher. This difference is very low and can be neglected.

Then, the MCM is applied to evaluate the relative standard deviation of  $Bl$ . It is assumed that the amplitudes  $U_1$  and  $S_1$  are uncorrelated. For each  $f_{sig}$ , Gaussian white noise with the standard deviation  $\sigma_{nu} = 0.1036$  mV and  $\sigma_{ns} = 1.8768$  nm are superimposed on the nominal points of  $\{u_i\}_{i=1}^{10^4}$  and  $\{s_i\}_{i=1}^{10^4}$ , respectively. Three algorithms are implemented to estimate the

amplitudes  $\hat{U}_1$  and  $\hat{S}_1$ , and then  $\hat{Bl}$  is determined. The process is repeated  $10^5$  times. The bias and the standard deviation of  $\hat{Bl}$  are calculated and presented in figure 4.

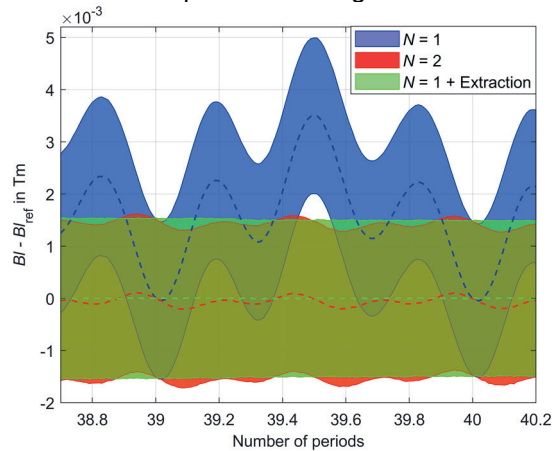


Figure 4: Bias and standard deviation of  $Bl$  estimated by the MCM. The dotted line represents the mean value of bias of  $Bl$  and the solid lines represent the confidence interval ( $k = 1$ ). The amplitudes are estimated by three-parameter sine fit (blue), multiharmonic sine fit ( $N = 2$ , red) and improved three-parameter sine fit (green).

As shown in figure 4, the three-parameter sine fit provides a bias of the  $Bl$  with non-coherent sampling, which is identical to the blue line in figure 2. Compared to the bias provided by the three-parameter sine fit, the influence of non-coherent sampling on the standard deviation can be neglected, even though the improved three-parameter sine fit acquires the highest standard deviation in figure 3. The results of the other two algorithms are almost identical. The multiharmonic sine fit with  $N = 2$  is comparable to the improved three-parameter sine fit in its stability.

Moreover, the relative standard deviation  $\sigma_{Bl_{rel}}$  determined by the GUF is compared with that provided by the MCM. The  $\sigma_{Bl_{rel}}$  is evaluated by Eq. (22), and it is assumed that the amplitudes  $U_1$  and  $S_1$  are uncorrelated. When using the MCM, the relative standard deviation  $\sigma_{\hat{Bl}_{rel}}$  is calculated by dividing the standard deviation  $\sigma_{\hat{Bl}}$  associated with  $\hat{Bl}$  by the reference value  $Bl_{ref}$ . As shown in figure 3, the  $\sigma_{Bl_{rel}}$  provided by the three-parameter and multiharmonic sine fit are indistinguishable, and thus only the latter one is presented in figure 5.

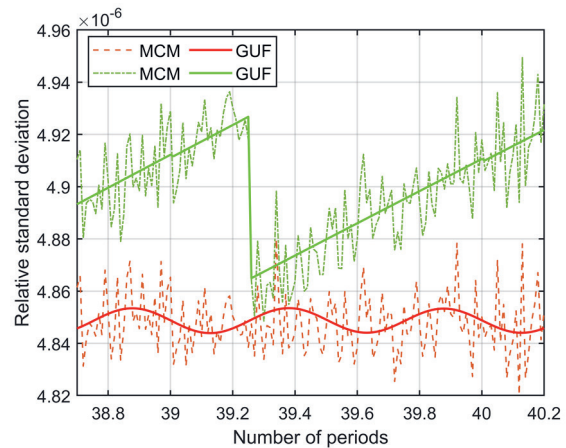


Figure 5: Relative standard deviation of  $Bl$  evaluated by the GUF and MCM, respectively. The amplitudes are estimated by multiharmonic sine fit ( $N = 2$ , red line) and improved three-parameter sine fit (green line).

In figure 5, the differences between  $\sigma_{Bl_{rel}}$  from the GUF and  $\sigma_{\hat{Bl}_{rel}}$  from the MCM are in the order of  $10^{-8}$  for each algorithm. The difference is two orders of magnitude smaller than the values of  $\sigma_{Bl_{rel}}$  and  $\sigma_{\hat{Bl}_{rel}}$ . Therefore, the results from GUF and MCM are comparable.

## Conclusion

In order to obtain a high accuracy of the force factor  $Bl$ , the relative bias and standard deviation of  $Bl$  are investigated in numerical simulations. When the sampled sine wave includes higher order harmonics with non-coherent sampling, the extraction of integer periods of the sine wave or multiharmonic sine fit can reduce the bias of the estimated amplitude, and further improve the accuracy of  $Bl$ . As for the standard uncertainty of  $Bl$ , the GUF and MCM are applied and the results of all the algorithms are comparable. In the future, other influences on the amplitude estimation, e.g. time jitter, quantization error, and numerical approximation, will also be investigated.

## Acknowledgement

The research of this project is funded via the program “Validierung des technologischen und gesellschaftlichen Innovationspotenzials – VIP+”, a program of the German Federal Ministry of Education and Research (BMBF), and is managed by VDI/VDE Innovation + Technik GmbH. The authors are grateful to members of Planck-Balance (PTB+TUIL) team for useful discussions.

## References

- [1] I. A. Robinson, S. Schlamminger, *Metrologia*, 53(5), A46-A74 (2016); doi: 10.1088/0026-1394/53/5/A46
- [2] C. Rothleitner, J. Schleichert, N. Rogge, L. Günther, S. Vasilyan, F. Hilbrunner, D. Knopf, T. Fröhlich, F. Härtig, *Measurement Science and Technology*, 29(7), 074003(2018); doi: 10.1088/1361-6501/aabc9e
- [3] J. Deyst, T. Sounders, O. Solomon, *IEEE Transactions on Instrumentation and Measurement*, 44(3), 637-642 (1995); doi: 10.1109/19.387298
- [4] P. M. Ramos, M. F. d. Silva, R. C. Martins, A. M. C. Serra, *IEEE Transactions on Instrumentation and Measurement*, 55(2), 646-651 (2006); doi: 10.1109/TIM.2006.864260
- [5] F. C. Alegria, *Measurement*, 42(5), 748-756 (2009); doi: 10.1016/j.measurement.2008.12.006
- [6] A. B. Forbes, in *Data Modeling for Metrology and Testing in Measurement Science*, Birkhäuser Boston, 147-176 (2008); doi: 10.1007/978-0-8176-4804-6\_5
- [7] BIPM, Evaluation of measurement data — Supplement 2 to the “Guide to the expression of uncertainty in measurement” — Extension to any number of output quantities, (2011).
- [8] C. Rothleitner, J. Schleichert, S. Vasilyan, N. Rogge, L. Günther, F. Hilbrunner, I. Rahneberg, D. Knopf, T. Fröhlich, F. Härtig, *Proc. of 2018 Conference on Precision Electromagnetic Measurements*, Paris, France, July 8-13 (2018); doi: 10.1109/CPEM.2018.8500904